A Novel Non-Orthogonal Multiple Access with Space-Time Line Codes for Massive IoT Networks

Ki-Hun Lee, Jeong Seon Yeom, and Bang Chul Jung
Department of Electronics Engineering
Chungnam National University
Daejeon, South Korea
Email: {kihun.h.lee; jsyeom; bcjung}@cnu.ac.kr

Jingon Joung
School of Electrical and Electronics Engineering
Chung-Ang University
Seoul, South Korea
Email: jgjoung@cau.ac.kr

***Abstract*—In this paper, we propose a novel uplink non-orthogonal multiple access (NOMA) for massive internet-of-things (IoT) networks where each device exploits a space-time line code (STLC) to send a small data packet to fusion center (FC) and the FC decodes the received packet without channel state information (CSI). In particular, we mathematically analyze the bit error ratio (BER) performance of the NOMA-based massive IoT network with the STLC by assuming the optimal joint maximum-likelihood (JML) detector. In addition, we propose a phase-steering based STLC (PS-STLC) technique to further improve the BER performance. Through extensive simulations, it is shown that the proposed PS-STLC technique achieves the optimal diversity and significantly improves the BER performance of the NOMA-based massive IoT network.**

***Index Terms*—Massive IoT networks, non-orthogonal multiple access (NOMA), BER, space-time line code (STLC), channel state information (CSI).**

I. Introduction

The internet-of-things (IoT) has received much attention from both academia and industry as one of the biggest technology trends. In particular, it is expected that over 25 billion IoT devices will be connected to cellular networks by 2020 [1]. In general, there exist massive connections in IoT networks and uplink traffic is much larger than downlink traffic. Thus, an efficient uplink multiple access protocol has been actively investigated in literature. The random access (RA) technique in the current cellular network like 3GPP LTE can be used for the uplink massive IoT networks; however, it suffers from preamble collision and overload problems as the number of IoT devices increases enormously even though several promising techniques have been proposed recently [2], [3].

On the other hand, a non-orthogonal multiple access (NOMA) [4], [5] has been considered as an emerging multiple access technique for the massive IoT network to overcome the limit of orthogonal multiple access (OMA) technique (e.g. orthogonal frequency division multiple access (OFDMA)) [6], [7]. The combined access protocol of the conventional RA and NOMA methods was also proposed in [8]–[11], where each device adjusts the transmit power such that the packet is received with a predetermined power level at a base station (BS) and the BS tries to decode them with a well-known successive interference cancellation (SIC) technique. The previous studies on the uplink NOMA systems employed the SIC technique at receivers [6]–[11], yet it was shown that the joint maximum-likelihood (JML) detector achieves the optimal performance for the uplink NOMA systems [12]. In addition, most existing studies on the NOMA techniques in the uplink massive IoT network have assumed that the channel state information (CSI) of each IoT device is known at the receiver (CSIR) [6]–[11]. However, if a large number of IoT devices simultaneously send their packet to a fusion center (FC), it is practically intractable for the FC to estimate the wireless channel of the devices especially with multiple antennas at the FC [7]. Instead, each device can estimate its channel to the FC by observing the pilot signal periodically broadcasted by the FC under the assumption of channel reciprocity.

In this paper, we propose a novel NOMA with space-time line code (STLC) for the uplink IoT network where the CSI of each device is unknown to the FC but it is known to each device. The STLC technique was proposed as a symmetric transmission scheme of the well-known space-time block code [13]. Recently, several variations of the STLC were proposed to improve communication performance without CSI at a receiver with multiple antennas [14]–[17]. We mathematically analyze the bit-error-rate (BER) performance of the proposed uplink NOMA system with the STLC. To further improve the performance of the uplink IoT network, we also propose a phase-steering based STLC (PS-STLC) technique. Simulation results reveal that the proposed PS-STLC significantly outperforms the STLC-based NOMA system without PS in terms of BER performance.

The remainder of this paper is organized as follows. In Section II, we introduce the system model considered in this paper. In Section III, we analyze the BER performance of uplink NOMA system with the STLC technique and validate the mathematical result though the computer simulations. In Section IV, we propose a PS-based STLC technique to improve the BER performance of the uplink NOMA system. Conclusion is drawn in Section V.

II. System Model

We consider an uplink IoT network with NOMA technique, where each IoT device is equipped with a single antenna and the FC is equipped with two antennas. In this paper, we focus

978-1-7281-1220-6/19/$31.00 ©2019 IEEE

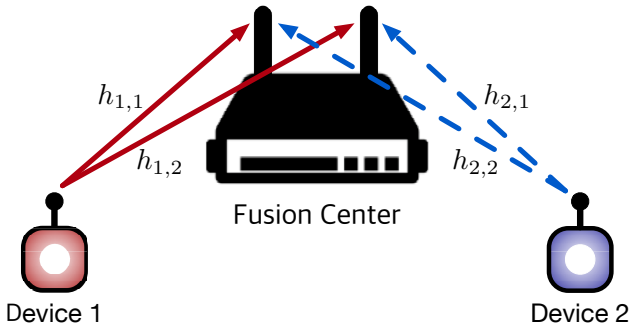

Fig. 1: Uplink IoT network with NOMA techniques.

on the case that *two* IoT devices share the same radio resource with the power-domain NOMA technique for convenience as shown in Fig. 1 even though more than *three* IoT devices can share the same radio resource in practice. Considering the random transmission nature of each IoT device and access control mechanisms, the case where two IoT devices share the same radio resource with NOMA technique will occur most frequently. It is assumed that the CSI between each IoT device and the FC is known at each IoT device by using the downlink pilot signal while the FC does not have the CSI [7]. It is also assumed that the transmitted symbol of each IoT device is modulated by the quadrature phase shift keying (QPSK) due to its power efficiency and low complexity. In addition, the information symbols of each IoT devices are encoded with the STLC by exploiting the local CSI for effectively obtaining spatial diversity. The STLC-encoded signals of the $n(\in\{1,2\})$-th IoT device at time slot $t(\in\{1,2\})$ is given by

$$s_{n,1}=\frac{h_{n,1}^{*}x_{n,1}+h_{n,2}^{*}x_{n,2}^{*}}{\sqrt{|h_{n,1}|^2+|h_{n,2}|^2}},\quad s_{n,2}=\frac{h_{n,2}^{*}x_{n,1}^{*}-h_{n,1}^{*}x_{n,2}}{\sqrt{|h_{n,1}|^2+|h_{n,2}|^2}}, \tag{1}$$

where $x_{n,t}$ and $h_{n,m}$ denote the QPSK modulated symbol of the n-th IoT device at the time slot t and the wireless channel coefficient between the n-th IoT device and the $m(\in\{1,2\})$-th receive antenna of the FC, respectively [13]. We assume that $\mathbb{E}\left[|x_{n,t}|^2\right]=\mathbb{E}\left[|s_{n,t}|^2\right]=1$ and $h_{n,m}$ follows identically and independently distributed (i.i.d) complex Gaussian distribution with zero mean and unit variance, i.e., $h_{n,m}\sim\mathcal{CN}(0,1)$.

Both IoT devices transmit STLC signals, $s_{n,1},\ s_{n,2}$, simultaneously during two time slots. Then, the received signal of two antennas at the FC during two time slots is given by

$$\begin{bmatrix}y_{1,1} & y_{1,2}\\ y_{2,1} & y_{2,2}\end{bmatrix}=\begin{bmatrix}\mathbf{h}_1 & \mathbf{h}_2\end{bmatrix}\begin{bmatrix}s_{1,1} & s_{1,2}\\ s_{2,1} & s_{2,2}\end{bmatrix}+\begin{bmatrix}w_{1,1} & w_{1,2}\\ w_{2,1} & w_{2,2}\end{bmatrix}, \tag{2}$$

where $y_{m,t}$ denotes the received signal at the m-th antenna at time slot t, $\mathbf{h}_n\triangleq[h_{n,1}\ h_{n,2}]^T$, and $w_{m,t}\sim\mathcal{CN}(0,N_0)$ denotes an noise at the m-th antenna at time slot t, respectively. The FC combines the received signals in (2) to obtain the original QPSK modulated symbols as follows [13]:

$$\begin{aligned}r_1&=y_{1,1}+y_{2,2}^{*}=\sqrt{\gamma_1}x_{1,1}+\sqrt{\gamma_2}x_{2,1}+w_{1,1}+w_{2,2}^{*},\\ r_2&=y_{2,1}^{*}-y_{1,2}=\sqrt{\gamma_1}x_{1,2}+\sqrt{\gamma_2}x_{2,2}+w_{2,1}^{*}-w_{1,2},\end{aligned} \tag{3}$$

QPSK Mapping Rule:

$00\rightarrow s_1=\frac{-1+j}{\sqrt{2}},\ 01\rightarrow s_2=\frac{-1-j}{\sqrt{2}},\ 10\rightarrow s_3=\frac{1+j}{\sqrt{2}},\ 11\rightarrow s_4=\frac{1-j}{\sqrt{2}}$

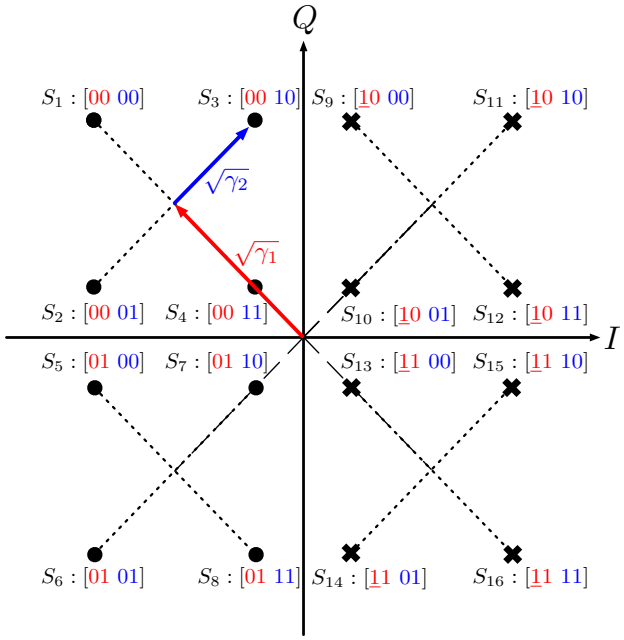

Fig. 2: Received signal constellation of superimposed QPSK symbols form two IoT devices when $\gamma_1\geq\gamma_2$.

where r_t is the estimate of the superimposed QPSK symbols of two IoT devices at time t and $\gamma_n\triangleq\|\mathbf{h}_n\|^2$. In this paper, it is assumed that the FC knows the effective channel gain γ_n by using the blind energy detection proposed in [17]. Then, the FC detects the signals $x_{n,t}$ by using joint maximum likelihood (JML) detection technique. Let a set of four QPSK symbol candidates be $\mathcal{X}$, i.e., $\mathcal{X}=\{s_1,s_2,s_3,s_4\}=\{(-1+j)/\sqrt{2},(-1-j)/\sqrt{2},(1+j)/\sqrt{2},(1-j)/\sqrt{2}\}$. The JML detection for the original QPSK symbols operates as follows:

$$[\hat{x}_{1,k},\hat{x}_{2,k}]=\underset{x_{1,k},x_{2,k}\in\mathcal{X}}{\arg\min}\ |r_k-\sqrt{\gamma}_1x_{1,k}-\sqrt{\gamma}_2x_{2,k}|^2, \tag{4}$$

where $k\in\{1,2\}$.

III. Performance Analysis of Uplink NOMA with Space-Time Line Codes

In this section, we mathematically analyze the BER performance of the uplink IoT network with STLC-based NOMA technique (STLC-NOMA). Let $b_{n,q}$ denote the $q(\in 1,2)$-th transmit bit of the n-th IoT device. Without loss of generality, we only consider the bit error case of the first bit of the first IoT device (i.e., $b_{1,1}$) since the other bit error cases can be analyzed with the same manner due to the symmetry. We assume $b_{1,1}=0$ as well. Fig. 2 shows the received signal constellation at the FC, which consists of two superimposed QPSK symbols, where S_i denotes the $i\in\{1,2,\ldots,16\}$-th constellation point. The mapping rule from two bits to a complex QPSK symbol is also given in Fig. 2. In Fig. 2, the

'$\circ$' marks represent the case that the first bit is equal to zero and the '$\times$' marks represent the bit error cases of the first bit.

In order to analyze the BER performance, we consider an error case with the minimum distance of the constellation. The BER of the first bit for given γ_1 and γ_2 is derived as follows:

$$\begin{aligned}&\Pr\{\mathcal{E} \mid \gamma_1, \gamma_2, b_{1,1}=0\}\\ &\quad\le \sum_{i=1}^{8} \Pr\{S_i \mid b_{1,1}=0\}\, Q\left(\sqrt{\frac{\delta_{i,\min}^2}{4N_0}}\right)\\ &\quad\overset{(a)}{=} \sum_{i=1}^{8} \frac{1}{8} Q\left(\sqrt{\frac{\delta_{i,\min}^2}{4N_0}}\right),\end{aligned} \tag{5}$$

where (a) follows from the fact that the probability that each QPSK modulated symbol is sent is symmetric; $\delta_{i,\min}$ denotes the Euclidean distance between the constellation point S_i and the nearest '$\times$' point from S_i. The constellation point S_i can be rewritten as $\sqrt{\gamma_1}s_{\lceil i/4\rceil} + \sqrt{\gamma_2}s_{((i-1) \bmod 4)+1}$. The distance $\delta_{i,\min}$ for $i = 1, 2, \ldots, 8$ can then be classified as follows:

$$\delta_{i,\min} = \begin{cases} \sqrt{2}\sqrt{\gamma_1}, & i = \{1,2,5,6\} \\ \sqrt{2}|\sqrt{\gamma_1} - \sqrt{\gamma_2}|, & i = \{3,4,7,8\} \end{cases} \tag{6}$$

We define the first case when $i = 1, 2, 5$, and 6 as a *outer* case $\mathcal{C}_{\mathsf{out}}$, and the second case when $i = 3, 4, 7$, and 8 as a *inner* case $\mathcal{C}_{\mathsf{in}}$. In the following subsections, we analyze the average BER performance of each case.

A. Outer Case

Let define a random variable $Y := \sqrt{\gamma_1} \triangleq \|\mathbf{h}_1\|$. The probability density function (PDF) of Y is then given by

$$f_Y(y) = 2y^3 e^{-y^2}. \tag{7}$$

The union bound for the error probability of the outer case is given by

$$\Pr\{\mathcal{E} \mid \gamma_1, \gamma_2, \mathcal{C}_{\mathsf{out}}\} \le \sum_{i\in\{1,2,5,6\}} \frac{1}{4} Q\left(\sqrt{\frac{\gamma_1}{2N_0}}\right), \tag{8}$$

and the upper bound of the average BER of the outer case is derived as follows:

$$\begin{aligned}\Pr\{\mathcal{E} \mid \mathcal{C}_{\mathsf{out}}\} &\le \mathbb{E}_Y\left[\sum_{i\in\{1,2,5,6\}} \frac{1}{4} Q\left(\sqrt{\frac{\gamma_1}{2N_0}}\right)\right]\\ &\le \frac{1}{4}\sum_{i\in\{1,2,5,6\}} \mathbb{E}_Y\left[Q\left(\sqrt{\frac{\gamma_1}{2N_0}}\right)\right]\\ &= \frac{1}{4}\sum_{i\in\{1,2,5,6\}} \int_0^\infty Q\left(\frac{y}{\sqrt{2N_0}}\right) f_Y(y)dy\\ &= \frac{1-\sqrt{4N_0+1}+(8-6\sqrt{4N_0+1})N_0+16N_0^2}{8(4N_0+1)^2}.\end{aligned} \tag{9}$$

B. Inner Case

Let define a random variable $Z := \left|\sqrt{\gamma_1} - \sqrt{\gamma_2}\right|^2$. The PDF of Z is the given by

$$\begin{aligned}f_Z(z) =& \frac{1}{64\sqrt{z}} e^{-z}\Big[2\sqrt{z}(z^2 - 4z + 15)\\ &- \sqrt{2\pi}e^{\frac{z}{2}}(z^3 - 3z^2 + 9z - 15)\mathrm{erfc}\left(\sqrt{\frac{z}{2}}\right)\Big].\end{aligned} \tag{10}$$

In order to derive the close-form BER expression of the inner case, we exploit the exponential bound of Q-function as follows [18]:

$$Q\left(\sqrt{\mu}\right) \le \frac{1}{2}\sum_{v=1}^{V} \alpha_v e^{-\beta_v \mu/2}, \tag{11}$$

where V is the iteration number related to the tighter upper bounds; $\alpha_v = 2(\lambda_v - \lambda_{v-1})/\pi$; $\beta_v = 1/\sin^2\lambda_v$; $\lambda_v = v\pi/2V$ for $v = 1, 2, ..., V$; and $\lambda_0 = 0$.

We now drive an exponential bound of the average BER of the inner case as follows:

$$\begin{aligned}\Pr\{\mathcal{E} \mid \mathcal{C}_{\mathsf{in}}\} &\le \mathbb{E}_Z\left[\sum_{i\in\{3,4,7,8\}} \frac{1}{4} Q\left(\sqrt{\frac{\left|\sqrt{\gamma_1} - \sqrt{\gamma_2}\right|^2}{2N_0}}\right)\right]\\ &= \frac{1}{4}\sum_{i\in\{3,4,7,8\}} \mathbb{E}\left[\frac{1}{2}\sum_{v=1}^{V} \alpha_v e^{-\beta_v\left|\sqrt{\gamma_1}-\sqrt{\gamma_2}\right|^2/4N_0}\right]\\ &= \frac{1}{8}\sum_{i\in\{3,4,7,8\}} \sum_{v=1}^{V} \alpha_v \mathbb{E}\left[e^{-\beta_v\left|\sqrt{\gamma_1}-\sqrt{\gamma_2}\right|^2/4N_0}\right]\\ &= \frac{1}{8}\sum_{i\in\{3,4,7,8\}} \sum_{v=1}^{V} \alpha_v \int_0^\infty e^{-\beta_v z/4N_0} f_Z(z)dz.\end{aligned} \tag{12}$$

In (12), the integration is derived as

$$\begin{aligned}\int_0^\infty e^{-\beta_v y/4N_0} f_Z(z)dz &= \frac{N_0(208N_0^2 + 104\beta_v N_0 + 15\beta_v^2)}{8(4N_0+\beta_v)^3}\\ &+ \frac{N_0^2(1216N_0^4 + 896\beta_v N_0^3 + 324\beta_v^2 N_0^2 + 78\beta_v^3 N_0 + 9\beta_v^4)}{4(2N_0+\beta_v)^3(4N_0+\beta_v)^3}\\ &+ \frac{3\beta_v(48N_0^2 + 24\beta_v N_0 + 5\beta_v^2)\tan^{-1}\sqrt{1+\frac{\beta_v}{2N_0}}}{16\sqrt{1+\frac{\beta_v}{2N_0}}(2N_0+\beta_v)^3}.\end{aligned} \tag{13}$$

C. Average BER

The average BER expression of the uplink STLC-NOMA system is obtained by using the total probability theorem as follows:

$$\begin{aligned}&\Pr\{\mathcal{E} \mid b_{1,1}=0\}\\ &\quad= \Pr\{\mathcal{E} \mid \mathcal{C}_{\mathsf{out}}\}\Pr\{\mathcal{C}_{\mathsf{out}} \mid b_{1,1}=0\}\\ &\qquad+ \Pr\{\mathcal{E} \mid \mathcal{C}_{\mathsf{in}}\}\Pr\{\mathcal{C}_{\mathsf{in}} \mid b_{1,1}=0\}\\ &\quad= \frac{1}{2}\left(\Pr\{\mathcal{C}_{\mathsf{out}} \mid b_{1,1}=0\} + \Pr\{\mathcal{C}_{\mathsf{in}} \mid b_{1,1}=0\}\right).\end{aligned} \tag{14}$$

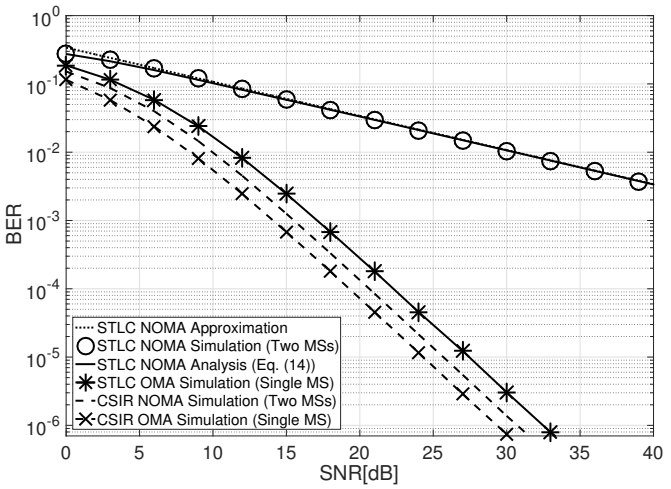

Fig. 3: Average BER performance of uplink STLC-NOMA and OMA systems.

Using (9) and (12) to (14), the approximated BER of the uplink STLC-NOMA in the high SNR regime can be expressed by using Taylor series as follows:

$$\Pr(\mathcal{E}) \approx \frac{15\pi}{64\sqrt{2}} \sum_{v=1}^{V} \frac{\alpha_v}{\sqrt{\beta_v}} N_0^{1/2}. \tag{15}$$

D. Numerical Results

Fig. 3 shows the average BER performance of the uplink STLC-NOMA system. The STLC OMA stands for the BER performance of the conventional STLC [13]. Somewhat surprisingly, the orthogonal multiple access (OMA) systems and the NOMA with CSIR achieve the optimal diversity while the uplink STLC-NOMA system does not achieve the optimal diversity. With the STLC, the minimum distance of constellation points of NOMA-STLC becomes smaller than that of the conventional NOMA with CSIR. Thus, the BER performance of the uplink NOMA with STLC technique becomes worse than the conventional techniques. Thus, we now propose a novel transmission technique to improve the BER performance of the NOMA system with STLC in the next section.

IV. Phase Steered STLC for Uplink NOMA

Before explaining the proposed phase steered STLC technique, it is worth noting that the characteristics of the uplink STLC-NOMA signals in (3). The QPSK symbols $x_{1,t}$ and $x_{2,t}$ are superimposed with the different magnitudes and the FC knows the effective channel gain γ_n. Based on these characteristics, we propose a simple but efficient transmission technique for each IoT device. To be specific, the QPSK symbols for two time slots of each IoT device are rotated by a certain angle and then encoded by the STLC. Here, the steering angle is independent of the channel gain ratio. Fig. 4 shows the received signal constellation of the proposed phase steered STLC (PS-SLTC) at the FC in the uplink NOMA system. Each device is assumed to receive the rotating angle θ_n ($0 < \theta_n < 90$) through the control signal from the FC. The PS coeffcient for two IoT devices are summarized in Table I.

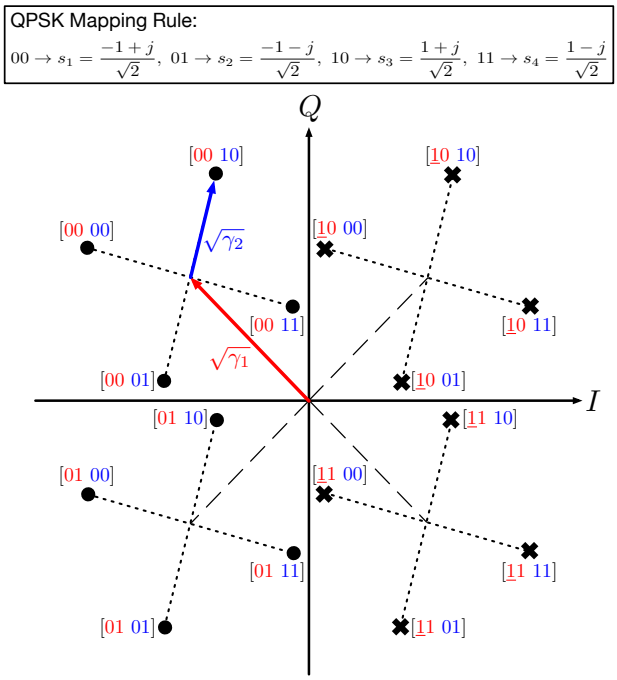

Fig. 4: Received signal constellation of superimposed QPSK symbols of the proposed PS-STLC NOMA, when $\gamma_1 \geq \gamma_2$.

In this paper, we assume that $\theta_1 = 0$ and $\theta_2 = \theta$ without loss of generality. In other words, only the QPSK symbols of the second IoT device are rotated by θ and them of the first IoT device are sent without any change.

TABLE I: Phase steering coefficients for two IoT devices

$x_{n,t}$	$t=1$	$t=2$
$n=1$	$e^{j\theta_1}$	
$n=2$	$e^{j\theta_2}$	

Defining the PS-STLC signals of the second IoT device as $s_{2,t}^{\text{PS}}$, they are given as follows:

$$\begin{aligned} s_{2,1}^{\text{PS}} &= \frac{h_{2,1}^* x_{2,1} e^{j\theta} + h_{2,2}^* x_{2,2}^* e^{-j\theta}}{\sqrt{\gamma_2}}, \\ s_{2,2}^{\text{PS}} &= \frac{h_{2,2}^* x_{2,1}^* e^{-j\theta} - h_{2,1}^* x_{2,2} e^{j\theta}}{\sqrt{\gamma_2}}, \end{aligned} \tag{16}$$

where The symbols of the first IoT device are the same as the symbols given in (1). Then, the received NOMA signals of the proposed PS-STLC at FC are given by

$$\begin{bmatrix} y_{1,1} & y_{1,2} \\ y_{2,1} & y_{2,2} \end{bmatrix} = \begin{bmatrix} \mathbf{h}_1 & \mathbf{h}_2 \end{bmatrix} \begin{bmatrix} s_{1,1} & s_{1,2} \\ s_{2,1}^{\text{PS}} & s_{2,2}^{\text{PS}} \end{bmatrix} + \begin{bmatrix} w_{1,1} & w_{1,2} \\ w_{2,1} & w_{2,2} \end{bmatrix}. \tag{17}$$

The FC performs the same linear combination for the received signals as in (17) as (3):

$$\begin{aligned} r_1^{\text{PS}} &= \sqrt{\gamma_1} x_{1,1} + \sqrt{\gamma_2} x_{2,1} e^{j\theta} + w_{1,1} + w_{2,2}^*, \\ r_2^{\text{PS}} &= \sqrt{\gamma_1} x_{1,2} + \sqrt{\gamma_2} x_{2,2} e^{j\theta} + w_{2,1}^* - w_{1,2}. \end{aligned} \tag{18}$$

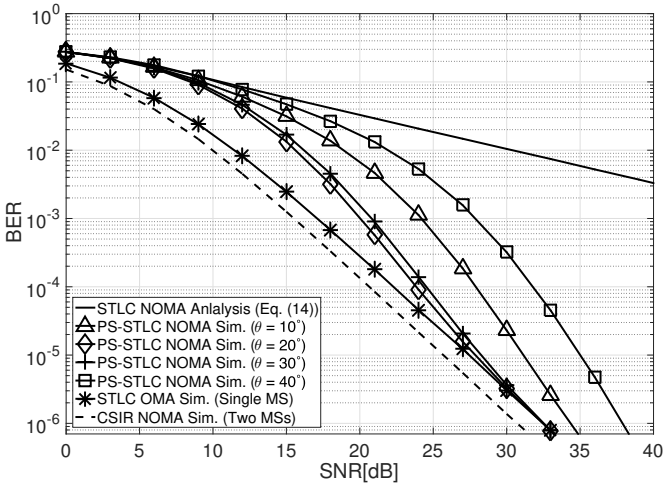

Fig. 5: Average BER performance of the proposed uplink PS-STLC NOMA and STLC-NOMA, and STLC OMA systems.

To detect the QPSK symbols of each device from (18), the FC adopts the JML detector with considering the PS coefficient:

$$[\hat{x}_{1,k}, \hat{x}_{2,k}] = \underset{x_{1,k}, x_{2,k} \in \mathcal{X}}{\arg\min} |r_k - \sqrt{\gamma_1} x_{1,k} - \sqrt{\gamma_2} x_{2,k} e^{j\theta}|^2. \tag{19}$$

Fig. 5 shows the BER performance of the proposed PS-STLC technique in the upink NOMA IoT network considering two devices. Interestingly, the proposed PS-STLC technique significantly improves the BER performance and even achieves the optimal diversity. We observe that the BER performance of the proposed PS-STLC technique varies according to the phase steering coefficient θ and thus the phase steering coefficient needs to be carefully controlled. Note that the BER performance of the PS-STLC technique with a proper PS coefficient approaches the performance of the STLC OMA system as the SNR increases, while increasing the spectral efficiency by two times.

V. Conclusion

We have proposed an uplink non-orthogonal multiple access (NOMA) with the space-time line code (STLC) for the IoT network, assuming each device has its channel state information (CSI), while the fusion center (FC) does not have it. We have mathematically analyzed the bit error rate (BER) performance of the STLC-based NOMA system in a closed-form expression. We have also proposed a novel STLC technique with phase-steering (PS-STLC), in which one of two devices rotates its constellation with a certain angle. Simulation results have verified that the proposed PS-STLC NOMA system significantly outperforms the STLC without PS and it achieves the optimal diversity gain as well. We leave the optimal steering phase design and its BER analysis for the PS-STLC in the uplink NOMA system as further studies.

Acknowledgment

This research was supported in part by the MSIT(Ministry of Science and ICT), Korea, under the ITRC(Information Technology Research Center) support program(IITP-2019-2017-0-01635) supervised by the IITP(Institute for Information & communications Technology Promotion), in part by the National Research Foundation of Korea (NRF) through the Basic Science Research Program funded by the Ministry of Science and ICT under Grant NRF-2019R1A2B5B01070697, and in part by the NRF grant funded by the Korea government (MSIT) (2018R1A4A1023826).

References

[1] Ericsson, "Cellular networks for massive IoT," tech. rep. Uen 284 23-3278, Jan. 2016; https://www.ericsson.com/res/docs/whitepapers/wp iot.pdf.

[2] H. S. Jang, H. Jin, B. C. Jung, and T. Q. S. Queck, "Versatile access control for massive IoT: Throughput, latency, and energy efficiency," *IEEE Trans. Mobile Comput.*, Apr. 2019 (early access article).

[3] H. Jin, W. T. Toor, B. C. Jung, and J. -B. Seo, "Recursive pseudo-bayesian access class barring for M2M communications in LTE systems," *IEEE Trans. Veh. Technol.*, vol. 66, no. 9, pp. 8595–8599, Sept. 2017.

[4] L. Dai, *et al.*, "Non-orthogonal multiple access for 5G: Solutions, challenges, opportunities, and future research trends," *IEEE Commun. Mag.*, vol. 53, no. 9, pp. 74–81, Sept. 2015.

[5] J. S. Yeom, E. Chu, B. C. Jung, and H. Jin, "Performance analysis of diversity-controlled multi-user superposition transmission for 5G wireless networks," *Sensors*, vol. 18, no. 2, p. 536, Feb. 2018.

[6] M. Shirvanimoghaddam, M. Condoluci, M. Dohler, and S. J. Johnson, "On the fundamental limits of random non-orthogonal multiple access in cellular massive IoT," *IEEE J. Sel. Areas Commun.*, vol. 35, no. 10, pp. 2238–2252, Oct. 2017.

[7] M. Shirvanimoghaddam, M. Dohler, and S. J. Johnson, "Massive non-orthogonal multiple access for cellular IoT: Potentials and limitations," *IEEE Commun. Mag.*, vol. 55, no. 9, pp. 55–61, Sept. 2017.

[8] J. -B. Seo, B. C. Jung, and H. Jin, "Nonorthogonal random access for 5G mobile communication systems," *IEEE Trans. Veh. Technol.*, vol. 67, no. 8, pp. 7867–7871, Aug. 2018.

[9] ——, "Performance analysis of NOMA random access," *IEEE Commun. Lett.*, vol. 22, no. 11, pp. 2242–2245, Nov. 2018.

[10] J. -B. Seo and B. C. Jung, "Random access games with cost of waiting for uplink NOMA systems," *IEEE Wireless Commun. Lett.*, May 2019 (early access article).

[11] J. -B. Seo, H. Jin, and B. C. Jung, "Multi-channel uplink NOMA random access: Selection diversity and bistability," *IEEE Commun. Lett.*, June 2019 (early access article).

[12] J. S. Yeom, H. S. Jang, K. S. Ko, and B. C. Jung (2018), "BER performance of uplink NOMA with joint maximum likelihood detector," Manuscript submitted for publication.

[13] J. Joung, "Space–time line code," *IEEE Access*, vol. 6, pp. 1023–1041, Feb. 2018.

[14] ——, "Space–time line code for massive MIMO and multiuser systems with antenna allocation," *IEEE Access*, vol. 6, pp. 962–979, Feb. 2018.

[15] ——, "Energy efficient space–time line coded regenerative two-way relay under per-antenna power constraints," *IEEE Access*, vol. 6, pp. 47026–47035, Sept. 2018.

[16] J. Joung and E. -R. Jeong, "Multiuser space–time line code with optimal and suboptimal power allocation methods," *IEEE Access*, vol. 6, pp. 51766–51775, Oct. 2018.

[17] J. Joung and B. C. Jung, "Machine learning based blind decoding for space–time line code (STLC) systems," *IEEE Trans. Veh. Technol.*, vol. 68, no. 5, pp. 5154–5158, May 2019.

[18] M. Chiani, D. Dardari, and M. K. Simon, "New exponential bounds and approximations for the computation of error probability in fading channels," *IEEE Trans. Wireless Commun.*, vol. 2, no. 4, pp. 840–845, July 2003.